

CutPaste&Find: Efficient Multimodal Hallucination Detector with Visual-aid Knowledge Base

Cong-Duy Nguyen¹ Xiaobao Wu^{1*} Duc Anh Vu¹
 Shuai Zhao¹ Thong Nguyen² Anh Tuan Luu^{1*}

¹Nanyang Technological University, Singapore

²National University of Singapore, Singapore

{nguyentr003, xiaobao.wu, vuducanh001, shuai.zhao, anhtuan.luu}@ntu.edu.sg
 thongnguyen050999@gmail.com

Abstract

Large Vision-Language Models (LVLMs) have demonstrated impressive multimodal reasoning capabilities, but they remain susceptible to hallucination, particularly object hallucination where non-existent objects or incorrect attributes are fabricated in generated descriptions. Existing detection methods achieve strong performance but rely heavily on expensive API calls and iterative LVLM-based validation, making them impractical for large-scale or offline use. To address these limitations, we propose CutPaste&Find, a lightweight and training-free framework for detecting hallucinations in LVLM-generated outputs. Our approach leverages off-the-shelf visual and linguistic modules to perform multi-step verification efficiently without requiring LVLM inference. At the core of our framework is a Visual-aid Knowledge Base that encodes rich entity-attribute relationships and associated image representations. We introduce a scaling factor to refine similarity scores, mitigating the issue of suboptimal alignment values even for ground-truth image-text pairs. Comprehensive evaluations on benchmark datasets, including POPE and R-Bench, demonstrate that CutPaste&Find achieves competitive hallucination detection performance while being significantly more efficient and cost-effective than previous methods.

1 Introduction

Large Vision Language Models (LVLMs) (Liu et al., 2023a; Ye et al., 2023; Zhu et al., 2023; Li et al., 2023a; Bai et al., 2023a; Dai et al., 2023b) have exhibited impressive multimodal understanding and reasoning abilities. They excel at various vision-language tasks, such as image captioning, visual question answering (VQA), and image-based dialogue, where they generate descriptive text based on visual inputs. For example, models such as LLaVA (Liu et al., 2023a)

	Number of time calling OpenAI api for 1 sentence	Module usage
Woodpecker	4	GroundDINO, BLIP2, QA2Claim
LogicCheckGPT	6	LVLM (MPlug)
Our	0	SGP, GroundDINO, BLIP2, CLIP

Table 1: Statistics of Calling OpenAI API and Module usage of LVLM hallucination detections.

and MiniGPT-4 (Zhu et al., 2023) can generate detailed captions from an image, answering complex questions about visual content. However, LVLMs face one critical challenge: object hallucination. This means LVLMs generate inconsistent or fabricated descriptions of a given image, such as inventing non-existent objects. This challenge undermines the reliability and accuracy of LVLMs, severely limiting their broader applications. To address this challenge, some hallucination detection methods have been proposed. For example, Woodpecker (Yin et al., 2023) is a training-free post-processing method that detects and corrects hallucinations in LVLMs. LogicCheckGPT (Wu et al., 2024a) is a plug-and-play framework that detects and mitigates object hallucinations in LVLMs by probing their logical consistency in responses.

"However, these methods have several limitations. First, they rely heavily on external API calls. As reported in Table 1, Woodpecker and LogicCheckGPT make 4-6 API calls to detect each sentence. This dependence also limits offline usability, making deployment infeasible in scenarios with restricted API access or privacy concerns. Second, they require iterative interactions with LVLMs to detect hallucinations. For instance, LogicCheckGPT generates multiple queries and performs consistency checks across responses. This iterative process not only increases latency but also amplifies token consumption, making it impractical for large-scale applications or real-time inference.

*Corresponding Authors.

To resolve these limitations, we propose a novel hallucination detection framework, CutPaste&Find. It is training-free, offline, and computationally efficient. Previous detection methods rely on external APIs. Differently, we validate visual entities with the pipeline by utilizing off-the-shelf textual and visual modules which are less hallucinated than LVLM (Yin et al., 2024). Moreover, we build a visual knowledge base to improve the reliability without high-computational interaction.

While these methods achieve strong performance, they are resource-intensive and costly due to frequent API calls and the computational overhead of LVLM inference. Moreover, they are not suitable for offline use. To address these limitations, we propose a novel framework called Cut-Paste&Find that is training-free, and efficient. Our framework leverages off-the-shelf modules to preprocess and perform multi-step inference without relying on powerful APIs.

Additionally, to further enhance our framework, we introduce a Visual-aid Knowledge Base as a robust solution for detecting multimodal hallucinations. Unlike traditional methods, our approach is grounded in a curated knowledge base built on human-annotated data, ensuring high accuracy and reliability. Specifically, this knowledge base is constructed through process called Cut-and-Paste using the Visual Genome dataset (Krishna et al., 2016), which incorporates rich information, including object names, attributes, relationships, and corresponding images.

The proposed method compares the visual representation similarity score of a cropped image (or the entire image) with entity-attribute pairs or triplet relations retrieved from the knowledge base. To improve the accuracy of alignment interpretation, we introduce a scaling factor with visual-aid prior knowledge. This innovation addresses the observation that similarity scores often deviate from ideal values near 1.0, even for ground-truth pairs. By incorporating this scaling factor, our framework refines similarity scores, enhancing their ability to represent true alignment between model outputs and the underlying image.

In summary, our main contributions are as follows:

- We propose a training-free, lightweight, and efficient framework named ABC for detecting hallucinations in LVLMs. This framework employs off-the-shelf modules to perform multi-step de-

tection with minimal resources and without reliance on costly APIs.

- We introduce a clean and robust Visual-aid Knowledge Base to enhance hallucination validation. This knowledge base integrates prior knowledge to improve detection accuracy.
- We evaluate the effectiveness of our framework through extensive experiments on benchmark datasets, including POPE (Li et al., 2023c) (with the split from (Wu et al., 2024a)) and R-Bench (Wu et al., 2024b). Our results demonstrate the robustness and efficiency of the proposed approach.

2 Related Work

2.1 LVLMs

With the rapid advancement of large language models (LLMs) (Ouyang et al., 2022; Zhao et al., 2023; Pan et al., 2024; Wu et al., 2024e,f,d,c), integrating their general intelligence into multimodal domains has garnered significant interest. This has led to the emergence of large vision-language models (LVLMs) (Ye et al., 2023; Zhu et al., 2023; Liu et al., 2023a; Li et al., 2023a; Dai et al., 2023a; Bai et al., 2023a), designed to understand and generate multimodal content under instructions. Most LVLMs adopt a two-stage training paradigm: multimodal alignment pre-training followed by instruction tuning, where an alignment module processes multimodal inputs before passing them to an LLM for response generation. For instance, mPLUG-Owl (Ye et al., 2023) pre-trains both the encoder and alignment module before fine-tuning LLaMa (Touvron et al., 2023) with low-rank adaptation. LLaVA (Liu et al., 2023a) pre-trains the alignment network and fine-tunes it alongside Vicuna (Chiang et al., 2023) on constructed instructions. In contrast, MiniGPT-4 (Zhu et al., 2023) only fine-tunes the cross-modal alignment network while keeping other components frozen.

2.2 Hallucination in LVLMs

Despite their strong capabilities, LVLMs often suffer from hallucination issues. To address this, several benchmarks (Fu et al., 2023; Xu et al., 2023; Yifan et al., 2023; Lovenia et al., 2023; Jing et al., 2023; Chen et al., 2024) have been proposed to evaluate hallucination severity in LVLMs. Existing mitigation strategies can be categorized into three groups. The first and most common approach (Liu et al., 2024; Gunjal et al., 2023; Lee et al., 2023;

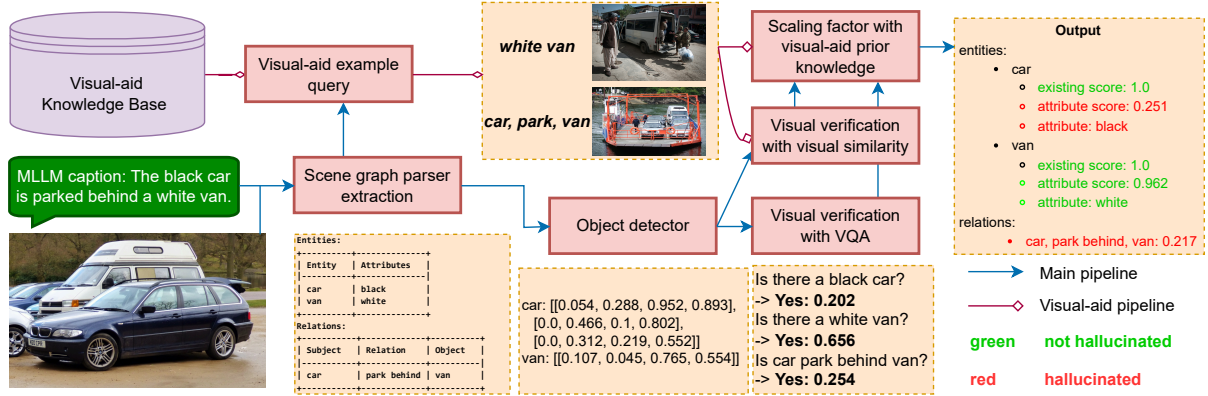


Figure 1: The overall architecture of CutPaste&Find. The system extracts scene graphs from captions, verifies object existence and attributes using a knowledge base, and employs object detection, visual similarity, and VQA for validation. A scaling factor adjusts similarity scores, enhancing reliability, with hallucinated entities and relations highlighted in red.

Wang et al., 2023) relies on instruction tuning and retraining. LRV-Instruction (Liu et al., 2024) constructs a diverse dataset with both positive and negative instructions, while (Wang et al., 2023) employs iterative instruction generation to enhance diversity and accuracy. Volcano (Lee et al., 2023) enables self-feedback training for response revision. However, these methods depend heavily on high-quality instruction datasets and require substantial computation. The second group focuses on decoding strategies to mitigate hallucinations. OPERA (Huang et al., 2023b) introduces a penalty-based decoding method with a rollback strategy to reduce overconfidence, while VCD (Leng et al., 2023) applies contrastive decoding to minimize reliance on spurious biases. However, accessing LVLMS’ internal states during decoding remains challenging for general users. The third category integrates external models to refine LVLMS outputs. Woodpecker (Yin et al., 2023) and LURE (Zhou et al., 2024) leverage external detectors or specialized LVLMS as revisors to improve visual understanding. However, these methods depend on auxiliary models rather than enhancing the base LVLMS itself. LogicCheckGPT (Wu et al., 2024a) takes a different approach by probing logical consistency in object-attribute relationships to detect and mitigate object hallucinations.

3 Method

In this section, we introduce the framework, first including Scene graph parser extraction, Object detector, Visual verification and then go through Scaling factor with visual-aid prior knowledge. We visualize the overall architecture in Figure 1.

3.1 Scene graph parser extraction

Captions often emphasize key concepts, and the first step in our framework involves extracting these concepts from the generated sentences. Unlike prior works that primarily focus on the main objects mentioned in a sentence, we extract entities alongside their attributes and the relationships between these entities. For example, given the sentence, “The man is wearing a black hat,” we extract entities (man, hat) and their attributes (black) and relationships (wearing). These serve as the foundation for subsequent hallucination diagnosis.

To achieve this, we leverage a Scene graph parser module (SGP), which efficiently converts unstructured textual descriptions into structured scene graphs. While large language models (LLMs) possess strong generalization capabilities and world knowledge, relying on them for this relatively straightforward task is resource-intensive and costly, particularly when APIs or open-source LLMs are used. SGP provides a more efficient alternative. Given a sentence s , SGP outputs two lists (a visualization is shown under Scene graph parser extraction in Figure 1):

$$E = [(e_1, a_1), (e_2, a_2), \dots] \quad (1)$$

$$R = [(s_1, r - 1, o_1), (s_2, r - 2, o_2), \dots] \quad (2)$$

e_i represents an entity and a_i represents its attribute (if applicable), (s_i, r_i, o_i) represents a relationship triplet of subject, relation, and object.

3.2 Object detector

Using the entities extracted by the SGP, we apply an open-set object detector (OD) to locate each

entity in the image. For a given entity e_i , if OD successfully detects it, we obtain a list of bounding boxes $B_i = \{b_{ia}, b_{ib}, \dots\}$, where each bounding box b_{ij} includes the top-left position (x, y) and dimensions (h, w) . If e_i cannot be detected, it is flagged as potentially hallucinated and validated using only the Visual Question Answering (VQA) module in the next step.

3.3 Visual verification

This stage validates the existence of entities, attributes, and relationships using two complementary methods: Visual Question Answering (VQA) and Visual Similarity.

3.3.1 Visual verification with VQA

We utilize a pre-trained VQA model (Li et al., 2023b) to answer context-specific questions about the image. Compared to LVLMs, the VQA model produces concise responses with fewer hallucinations, making it a suitable choice. We formulate three types of questions:

Attribute asking Given the entity e_i and attribute a_i , we ask the VQA model “Is the $\{e_i\}\{a_i\}$?”.

Relation asking Given the triplet s_i, r_i, o_i , we ask the VQA model “Is the $\{s_i\}\{r_i\}\{o_i\}$?”.

Existance asking This format is used when the entity e_i was missed from previous step 3.2. Given the entity e_i , we ask the VQA model “Is there $\{s_i\}$ in the image”.

We ask the VQA model in a binary Yes/No question, and instead of using the generated answer (“yes” or “no”), we base it on the scoring of “yes” token of the predicted probabilities of the output. Thus we can have a soft-predicted score s_i^{qa} instead of a hard prediction. Instead of relying on the binary outputs (yes or no), we use the probability of the yes token to derive a soft-predicted score s_i^{qa} , offering a more nuanced assessment.

3.3.2 Visual verification with Visual Similarity

To complement VQA, we validate hallucination using Visual-aid Knowledge Base. For an entity-attribute pair (a_i, e_i) , we retrieve a list of representative images \hat{C}_i from the datastore and compute visual representations f_i (for the cropped image) and \hat{F}_i (for retrieved images) using a pre-trained visual encoder (e.g., CLIP). The similarity score s_i^v is calculated between f_i and \hat{F}_i ; lower scores

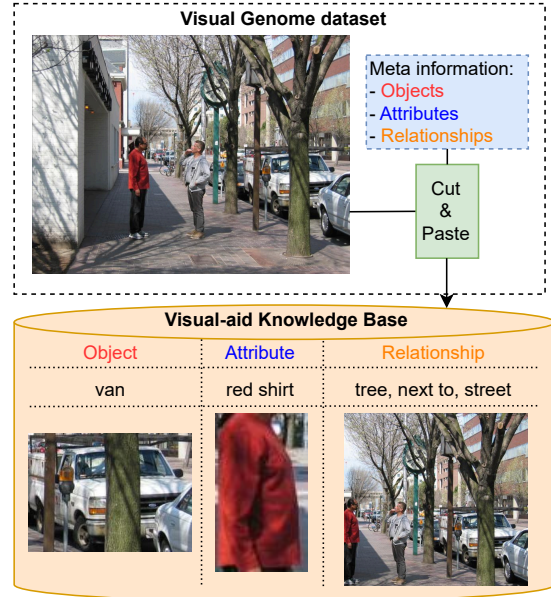


Figure 2: The figure illustrates a Visual-aid Knowledge Base built from meta-information and images, including objects, attributes, and relationships. A “Cut & Paste” process segments visual elements such as objects (e.g., van), attributes (e.g., red shirt), and relationships (e.g., tree next to street) into a structured knowledge base.

indicate higher likelihoods of hallucination. A similar approach is applied to validate relationships s_i, r_i, o_i .

3.4 Scaling factor with Visual-aid prior knowledge

Similarity scores often deviate from ideal values near 1.0, even for ground-truth pairs. To address this, we introduce a scaling factor derived from the prior knowledge embedded in the datastore. This adjustment aligns similarity scores with realistic expectations, improving the sensitivity and robustness of hallucination detection.

Visual Scaling Factor The scaling factor for visual encoding is computed as:

$$\tilde{S}_i^v = f(\hat{F}_i, \hat{F}_i^\top) \quad (3)$$

$$\text{diag}(\tilde{S}_i^v) = 0 \quad (4)$$

$$d_i^v = \max(\tilde{S}_i^v) \quad (5)$$

where d_i^v is the scaling factor for the visual encoding method. Then we calculate re-scale similarity score of an entity e_i :

$$\bar{s}_i^v = s_i^v / d_i^v \quad (6)$$

VQA Scaling Factor For the VQA module, we compute the scaling factor:

$$\tilde{S}_i^{qa} = [\tilde{s}_{i1}^{qa}, \tilde{s}_{i2}^{qa}, \dots, \tilde{s}_{ij}^{qa}] \quad (7)$$

$$\text{diag}(\tilde{S}_i^{qa} a_i) = 0 \quad (8)$$

$$d_i^{qa} = \max(\tilde{S}_i^{qa}) \quad (9)$$

where d_i^{qa} is the scaling factor for the visual question module. Then we calculate the re-scale similarity score of an entity e_i :

$$\bar{s}_i^{qa} = s_i^{qa} / d_i^{qa} \quad (10)$$

Final output Given a generated caption s and an image I , our classifier outputs a hallucination dictionary:

- Entity: $[e_1 : \tilde{s}_{e1}, \dots, e_i : \tilde{s}_{ei}]$
- Attribute-entity: $[e_1, a_1 : \tilde{s}_{a1}, \dots, e_i, a_i : \tilde{s}_{ai}]$
- Relation: $[s_1, r_1, o_1 : \tilde{s}_{r1}, \dots, s_j, r_j, o_j : \tilde{s}_{ri}]$

where s_e, s_a, s_r are the existing, attribute, and relation score respectively. This structured output enables precise identification and correction of hallucinations, ensuring multimodal consistency.

4 Visual-aid Knowledge Base

4.1 Cut-And-Paste

Our Visual-aid Knowledge Base (VaKB) is built upon the Visual Genome dataset, a rich resource for tasks requiring fine-grained visual understanding. The VG includes 101,174 images sourced from MSCOCO, accompanied by 1.7 million question-answer pairs, averaging 17 questions per image. Unlike the traditional VQA datasets, Visual Genome offers a balanced distribution of six question types: What, Where, When, Who, Why, and How, making it particularly suitable for diverse multimodal reasoning tasks. Furthermore, it provides 108,000 images densely annotated with objects, attributes, and relationships, making it an invaluable resource for constructing comprehensive knowledge bases that bridge visual and textual modalities. We will pre-process the dataset with its annotation through process call "Cut-And-Paste".

4.2 Datastore

Each image I in the Visual Genome dataset is enriched with human annotations, including entities, attributes, and relationships. These annotations are structured as follows:

Method	Acc	Precision	Recall	F1 Score
<i>Adversarial</i>				
Woodpecker $^\diamond$	90.67	90.13	91.33	90.73
LC-GPT $^\diamond$	83.33	94.64	70.67	80.92
CutPaste&Find	94.67	92.95	96.67	94.77
<i>Popular</i>				
Woodpecker $^\diamond$	89.67	91.03	88.00	89.49
LC-GPT $^\diamond$	85.00	94.87	74.00	83.15
CutPaste&Find	93.67	93.96	93.33	93.65
<i>Random</i>				
Woodpecker $^\diamond$	93.33	94.52	92.00	93.24
LC-GPT $^\diamond$	85.67	98.20	72.67	83.52
CutPaste&Find	95.67	95.36	96.00	95.68

Table 2: Results on POPE. The best performances within each setting are **bolded**. $^\diamond$ We run these models using the OpenAI GPT-4o version. Instead of passing non-existent claims as done in their implementation, we convert all yes-no questions into affirmative statements.

Entities Each entity includes the object name and its bounding box in (x, y, w, h) format.

Attributes Each entity is further extended with a list of associated attributes, providing additional descriptive detail.

Relationships Each relationship annotation is represented as a triplet (s, r, o) , where s is the subject, r is the relationship, and o is the object.

To build the VaKB, we crop the bounding boxes of entities and store both the cropped and original images in a database. This ensures that for each key k , we have a list of cropped images and their corresponding full images. Keys are constructed from entities, attribute-entity pairs, and relationship triplets. Formally, we define the datastore as a collection of key-value pairs (k_i, v_i) , where the key k_i can represent an entity e_i , an attribute-entity pair (e_i, a_i) , or a relationship triplet (s_i, r_i, o_i) . The value v_i consists of the associated cropped and original images. To facilitate retrieval, each key k_i is mapped to a fixed-length vector representation $f^T(k_i)$, computed by a pre-trained text encoder (e.g., CLIP-Text). The datastore $(\mathcal{K}, \mathcal{V})$ is constructed as:

$$(\mathcal{K}, \mathcal{V}) = \{(f^T(k_i), v_i) | (k_i, v_i) \in \mathcal{D}, \quad (11)$$

$$k_i \in \{e_i, (e_i, a_i), (s_i, r_i, o_i)\} \} \quad (12)$$

Here, \mathcal{D} represents the annotated examples in the Visual Genome dataset.

Method	Acc	Precision	Recall	F1 Score
<i>Image level</i>				
Woodpecker [◇]	55.00	55.03	54.67	54.85
LC-GPT [◇]	62.00	66.07	49.33	56.49
CutPaste&Find	79.00	74.58	88.00	80.73
<i>Instance level</i>				
Woodpecker [◇]	56.67	57.04	54.00	55.48
LC-GPT [◇]	60.67	62.12	54.67	58.16
CutPaste&Find	72.33	66.67	89.33	76.35

Table 3: Results on RBench. The best performances within each setting are **bolded**. [◇] We run these models using the OpenAI GPT-4o version. Instead of passing non-existent claims as done in their implementation, we convert all yes-no questions into affirmative statements.

5 Experiment

5.1 Experimental Settings

5.1.1 Benchmark

POPE (Yifan et al., 2023): POPE evaluates hallucinations in LVLMs using three sampling strategies: random, popular, and adversarial, each differing in negative sample construction. The random strategy selects objects absent from the image, popular samples frequent but non-existent objects, and adversarial picks commonly co-occurring but missing objects. Following (Li et al., 2023c), we sampled 50 images, generating six questions per image with an equal mix of positive and negative samples (50%). Object annotations were converted into binary Yes-or-No questions, focusing on existence hallucinations. LVLMs determine object presence, with performance measured via accuracy, precision, recall, and F1-score.

R-Bench (Wu et al., 2024b): The Relationship Hallucination Benchmark (R-Bench) evaluates relationship hallucinations in LVLMs. It comprises 11,651 binary questions: 7,883 image-level for global relationships and 3,768 instance-level for localized ones, using bounding boxes or masks. Evaluations on popular LVLMs reveal relationship hallucinations are more prevalent than object-level ones due to long-tail distributions and co-occurrence biases, highlighting challenges in spatial reasoning and reliance on commonsense over visual cues. R-Bench promotes improvements in mitigating relationship hallucinations via fine-grained image-text alignment.

5.1.2 Implementation

Baselines. We choose mainstream LVLMs as our baseline models, including mPLUG-Owl (Ye et al.,

2023), LLaVA (Liu et al., 2023b), Qwen (Bai et al., 2023b). Regarding LVLm hallucination detection, we compare our work with Woodpecker (Yin et al., 2023) and LogicCheckGPT (LCGPT) (Wu et al., 2024a).

Implementation Details. Our pipeline is training-free and comprises several pre-trained models apart from the LVLm to be corrected.

- Scene Graph Parser: we use FlanT5 pretrained with FACTUAL (Li et al., 2023d) to extract textual scene graph.
- Open-set object detection: we use Grounding DINO (Liu et al., 2023c) to extract object counting information with default detection thresholds.
- Textual encoder, visual encoder: we use pre-trained CLIP (Radford et al., 2021) for extracting text and visual representation.
- Visual question answering: we use BLIP-2-FlanT5_{XXL} (Li et al., 2023b) as the VQA model to answer the question about: existence, attribute, and relation.
- Datastore: To search over this large datastore, we use FAISS (Johnson et al., 2017), an open-source library for fast nearest neighbor retrieval in high dimensional spaces.

For both POPE and R-Bench benchmark, they are both “Yes-or-No” questions, instead of feeding the question and the answer from LVLMs, we use QA2Claim model (Huang et al., 2023a) to convert all questions into claims which assume the answer is “Yes”. For example, given a question, “Is there a dog in the image?”, we convert into the specific caption “There is a dog in the image.”.

5.2 Experimental Results

5.2.1 POPE

Table 2 presents the performance of all methods across the different data splits. Our method consistently outperforms both baselines in all metrics and data splits, demonstrating superior robustness and generalization capabilities.

Adversarial Split In the adversarial split, which challenges the models with difficult examples designed to exploit their weaknesses, our method achieves an Accuracy of 94.67%, surpassing Woodpecker (90.67%) and Logic (83.33%). Notably, our

method maintains a high Precision of 92.95% and an outstanding Recall of 96.67%, leading to the highest F1 Score of 94.77%. This indicates that our model is not only accurate but also reliable in identifying true positives even under adversarial conditions.

Popular Split For the popular split, which includes frequently occurring patterns, our method achieves an Accuracy of 93.67%, significantly higher than Woodpecker (89.67%) and Logic (85.00%). The F1 Score of 93.65% highlights our method’s balanced performance in terms of Precision (93.96%) and Recall (93.33%), confirming its effectiveness in handling common data patterns without overfitting.

Random Split In the random split, designed to reflect general, unbiased data distribution, our method achieves the highest Accuracy of 95.67%, outperforming Woodpecker (93.33%) and Logic (85.67%). With a Precision of 95.36% and Recall of 96.00%, our method attains an exceptional F1 Score of 95.68%, demonstrating its strong generalization capability across diverse data samples.

5.2.2 R-Bench

Table 3 summarizes the performance of all methods on the R-Bench benchmark, evaluated at both the image and instance levels. Our method consistently demonstrates superior performance, underscoring its robustness and adaptability across different granularity levels.

Image Level At the image level, our method achieves an Accuracy of 79.00%, significantly outperforming Woodpecker (55.00%) and Logic (62.00%). The Precision of 74.58% and outstanding Recall of 88.00% lead to the highest F1 Score of 80.73%. These results highlight our model’s effectiveness in accurately identifying relevant features within images.

Instance Level For instance-level evaluation, our method achieves an Accuracy of 72.33%, compared to Woodpecker (56.67%) and Logic (60.67%). The Precision of 66.67% and remarkable Recall of 89.33% result in an F1 Score of 76.35%, indicating our model’s strong capability to generalize well at a finer granularity, effectively capturing individual instances within images.

6 Ablation study

To further validate our approach, we conducted an extensive evaluation using the full POPE dataset

Method	Acc	Precision	Recall	F1 Score
<i>Adversarial</i>				
LLaVA	50.77	50.39	99.87	66.98
mPLUG-Owl	50.67	50.34	99.33	66.82
CutPaste&Find	81.26	77.92	87.27	82.33
<i>Popular</i>				
LLaVA	52.43	51.25	99.80	66.79
mPLUG-Owl	50.63	50.32	99.27	67.72
CutPaste&Find	89.83	91.99	87.27	89.57
<i>Random</i>				
LLaVA	54.43	52.32	99.80	68.65
mPLUG-Owl	53.30	51.71	99.53	68.06
CutPaste&Find	86.80	86.46	87.27	86.86

Table 4: Results on POPE (Full version). The best performances within each setting are **bolded**.

(9000 samples), and the results are presented in Table 2. Our method is compared against two additional state-of-the-art models: LLaVA and mPLUG-Owl.

Random Split Our method achieves an Accuracy of 86.80%, significantly outperforming LLaVA (54.43%) and mPLUG-Owl (53.30%). The Precision of 86.46% and Recall of 87.27% lead to the highest F1 Score of 86.86%, demonstrating strong generalization across randomly distributed samples.

Popular Split For the popular split, our method again achieves superior performance with an Accuracy of 89.83%, compared to LLaVA (52.43%) and mPLUG-Owl (50.63%). The F1 Score of 89.57% highlights our model’s ability to capture frequently occurring patterns while maintaining high precision (91.99%) and recall (87.27%).

Adversarial Split In the adversarial setting, which is particularly challenging, our method maintains an Accuracy of 81.26%, a substantial improvement over LLaVA (50.77%) and mPLUG-Owl (50.67%). The F1 Score of 82.33% further confirms its robustness, balancing Precision (77.92%) and Recall (87.27%).

6.1 Experiment on full POPE

To highlight the necessity of our scaling factor, we analyze similarity scores in the visual-aid knowledge base. As shown in Table 4, ground-truth validation images often receive suboptimal similarity scores despite correctly representing the queried object. For example, a wooden medicine cabinet scores 0.558, with alternative images varying from 0.383 to 0.805. Similarly, white fridge and train on track validation images score 0.922 and 0.655,

while some alternatives score even higher (e.g., 0.823 for white fridge and 0.845 for train on track), despite contextual differences. These inconsistencies suggest that raw similarity scores may not fully capture object fidelity, leading to misinterpretations in hallucination detection. Our scaling factor mitigates this by incorporating prior knowledge from the datastore, aligning scores with realistic expectations and improving hallucination sensitivity.

6.2 VQA scoring visualization

To illustrate the necessity of our scaling factor, we analyze similarity scores in the visual-aid knowledge base. As shown in Figure 5, ground-truth validation images often receive lower-than-ideal similarity scores despite correctly representing the queried object. For example, a wooden medicine cabinet scores 0.558, while alternative images range from 0.383 to 0.805. Similarly, white fridge and train on track validation images score 0.922 and 0.655, yet some alternative images score even higher (e.g., 0.823 and 0.845, respectively), despite contextual differences. These inconsistencies indicate that raw similarity scores do not fully capture object fidelity, leading to misinterpretations in hallucination detection. Our scaling factor mitigates this by incorporating prior knowledge from the datastore, aligning scores with realistic expectations and improving sensitivity to hallucinations.

6.3 Visualization

6.3.1 Open-set Object detector based comparison

The qualitative examples in Figure 3 demonstrate our model’s effectiveness in detecting hallucinations, particularly where Woodpecker generates incorrect or misleading responses. In the first case, when asked about a sports ball, Woodpecker incorrectly states that none is present, while our model correctly identifies it with an existence score of 1.0, avoiding the hallucination of a missing entity. Similarly, for a dining table, Woodpecker misidentifies a generic table, whereas our model assigns an existence score of 0.0, accurately detecting the hallucination. In the black leather couch example, Woodpecker detects a couch but fails to confirm its leather attribute, creating ambiguity. Our model explicitly identifies the leather attribute with high confidence (0.9228) and captures relational understanding by confirming the woman’s sitting position with a score of 0.9431, which Woodpecker lacks. Lastly, for the smiling baby, Woodpecker

falsely asserts the baby is smiling, while our model assigns a lower smiling attribute score (0.3378), reflecting uncertainty and mitigating hallucinated affirmations. These examples highlight our model’s robustness in leveraging existence, attribute confidence scores, and relational reasoning to mitigate hallucinations, outperforming Woodpecker in multimodal verification.

6.3.2 Failed cases

The examples in Figure 4 illustrate failure cases where our model struggles with complex language structures, particularly in fine-grained attributes and relational constraints. In the first case, the question asks whether there are trees without lights outside a strip mall. While our model correctly detects trees and the strip mall (existence score: 1.0) and their spatial relationship (0.8866), it fails to distinguish decorated from undecorated trees, revealing a limitation in attribute-based reasoning for multi-condition queries. In the second case, the question asks whether two women are playing table tennis against each other. The model detects women and table tennis (existence score: 1.0) and identifies the women, play, table tennis relation (0.6176). However, it fails to capture the against each other condition, requiring a deeper understanding of competitive interactions rather than simple activity recognition. These cases highlight our model’s difficulty with compositional language, negation, and multi-entity interactions. To overcome these limitations, improvements in linguistic grounding and multimodal reasoning are needed to better handle complex queries.

7 Conclusion

In this work, we introduced CutPaste&Find, a novel, training-free framework for detecting hallucinations in LVLN-generated descriptions. Unlike existing methods that depend on costly LVLN-based inference, our approach utilizes off-the-shelf visual and linguistic tools, making it both efficient and scalable. By incorporating a visual-aid knowledge base and a scaling factor for improved similarity alignment, our method enables robust hallucination detection with minimal computational overhead. Experimental results on benchmark datasets demonstrate that CutPaste&Find is both effective and resource-efficient, offering a practical solution for enhancing the reliability of LVLNs.

Limitations

The proposed method relies heavily on the Visual Genome dataset for constructing its visual-aid knowledge base, which limits its generalizability to domains lacking high-quality, well-annotated datasets. Expanding to domain-specific or low-resource scenarios may require significant manual effort to curate new knowledge bases. Additionally, while the approach effectively verifies object existence, attributes, and relations, it struggles with fine-grained semantic understanding, particularly in handling compositional queries, negations, and multi-entity interactions. For instance, it may fail to distinguish between "two women playing against each other" and simply "playing table tennis," highlighting a limited ability to process intricate logical dependencies in multimodal reasoning.

References

- Jinze Bai, Shuai Bai, Shusheng Yang, Shijie Wang, Sinan Tan, Peng Wang, Junyang Lin, Chang Zhou, and Jingren Zhou. 2023a. Qwen-vl: A frontier large vision-language model with versatile abilities. *arXiv preprint arXiv:2308.12966*.
- Jinze Bai, Shuai Bai, Shusheng Yang, Shijie Wang, Sinan Tan, Peng Wang, Junyang Lin, Chang Zhou, and Jingren Zhou. 2023b. Qwen-vl: A versatile vision-language model for understanding, localization, text reading, and beyond. *arXiv*.
- Xiang Chen, Chenxi Wang, Yida Xue, Ningyu Zhang, Xiaoyan Yang, Qiang Li, Yue Shen, Jinjie Gu, and Huajun Chen. 2024. Unified hallucination detection for multimodal large language models. *arXiv preprint arXiv:2402.03190*.
- Wei-Lin Chiang, Zhuohan Li, Zi Lin, Ying Sheng, Zhanghao Wu, Hao Zhang, Lianmin Zheng, Siyuan Zhuang, Yonghao Zhuang, Joseph E Gonzalez, et al. 2023. Vicuna: An open-source chatbot impressing gpt-4 with 90%* chatgpt quality. See <https://vicuna.lmsys.org> (accessed 14 April 2023).
- W Dai, J Li, D Li, AMH Tiong, J Zhao, W Wang, B Li, P Fung, and S Hoi. 2023a. Instructblip: Towards general-purpose vision-language models with instruction tuning. *arXiv preprint arXiv:2305.06500*.
- Wenliang Dai, Junnan Li, Dongxu Li, Anthony Meng Huat Tiong, Junqi Zhao, Weisheng Wang, Boyang Li, Pascale Fung, and Steven Hoi. 2023b. Instructblip: Towards general-purpose vision-language models with instruction tuning. *arXiv preprint arXiv:2305.06500*.
- Chaoyou Fu, Peixian Chen, Yunhang Shen, Yulei Qin, Mengdan Zhang, Xu Lin, Jinrui Yang, Xiawu Zheng, Ke Li, Xing Sun, et al. 2023. Mme: A comprehensive evaluation benchmark for multimodal large language models. *arXiv preprint arXiv:2306.13394*.
- Anisha Gunjal, Jihan Yin, and Erhan Bas. 2023. Detecting and preventing hallucinations in large vision language models. *arXiv*.
- Kung-Hsiang Huang, Hou Pong Chan, and Heng Ji. 2023a. Zero-shot faithful factual error correction. In *Proceedings of the 61st Annual Meeting of the Association for Computational Linguistics (Volume 1: Long Papers)*, pages 5660–5676, Toronto, Canada. Association for Computational Linguistics.
- Qidong Huang, Xiaoyi Dong, Pan Zhang, Bin Wang, Conghui He, Jiaqi Wang, Dahua Lin, Weiming Zhang, and Nenghai Yu. 2023b. Opera: Alleviating hallucination in multi-modal large language models via over-trust penalty and retrospection-allocation. *arXiv preprint arXiv:2311.17911*.
- Liqiang Jing, Ruosen Li, Yunmo Chen, Mengzhao Jia, and Xinya Du. 2023. Faithscore: Evaluating hallucinations in large vision-language models. *arXiv preprint arXiv:2311.01477*.
- Jeff Johnson, Matthijs Douze, and Hervé Jégou. 2017. Billion-scale similarity search with gpus. *arXiv preprint arXiv:1702.08734*.
- Ranjay Krishna, Yuke Zhu, Oliver Groth, Justin Johnson, Kenji Hata, Joshua Kravitz, Stephanie Chen, Yannis Kalantidis, Li-Jia Li, David A. Shamma, Michael S. Bernstein, and Fei-Fei Li. 2016. Visual genome: Connecting language and vision using crowdsourced dense image annotations. *Preprint*, arXiv:1602.07332.
- Seongyun Lee, Sue Hyun Park, Yongrae Jo, and Minjoon Seo. 2023. Volcano: mitigating multimodal hallucination through self-feedback guided revision. *arXiv preprint arXiv:2311.07362*.
- Sicong Leng, Hang Zhang, Guanzheng Chen, Xin Li, Shijian Lu, Chunyan Miao, and Lidong Bing. 2023. Mitigating object hallucinations in large vision-language models through visual contrastive decoding. *arXiv preprint arXiv:2311.16922*.
- Bo Li, Yuanhan Zhang, Liangyu Chen, Jinghao Wang, Jingkang Yang, and Ziwei Liu. 2023a. Otter: A multi-modal model with in-context instruction tuning. *arXiv preprint arXiv:2305.03726*.
- Junnan Li, Dongxu Li, Silvio Savarese, and Steven Hoi. 2023b. Blip-2: Bootstrapping language-image pre-training with frozen image encoders and large language models. *arXiv*.
- Yifan Li, Yifan Du, Kun Zhou, Jinpeng Wang, Wayne Xin Zhao, and Ji-Rong Wen. 2023c. Evaluating object hallucination in large vision-language models. *arXiv*.

- Zhuang Li, Yuyang Chai, Terry Yue Zhuo, Lizhen Qu, Gholamreza Haffari, Fei Li, Donghong Ji, and Quan Hung Tran. 2023d. [FACTUAL: A benchmark for faithful and consistent textual scene graph parsing](#). In *Findings of the Association for Computational Linguistics: ACL 2023*, pages 6377–6390, Toronto, Canada. Association for Computational Linguistics.
- Fuxiao Liu, Kevin Lin, Linjie Li, Jianfeng Wang, Yaser Yacoob, and Lijuan Wang. 2024. Mitigating hallucination in large multi-modal models via robust instruction tuning. *ICLR*.
- Haotian Liu, Chunyuan Li, Qingyang Wu, and Yong Jae Lee. 2023a. Visual instruction tuning. In *NeurIPS*.
- Haotian Liu, Chunyuan Li, Qingyang Wu, and Yong Jae Lee. 2023b. Visual instruction tuning. *arXiv*.
- Shilong Liu, Zhaoyang Zeng, Tianhe Ren, Feng Li, Hao Zhang, Jie Yang, Chunyuan Li, Jianwei Yang, Hang Su, Jun Zhu, et al. 2023c. Grounding dino: Marrying dino with grounded pre-training for open-set object detection. *arXiv*.
- Holy Lovenia, Wenliang Dai, Samuel Cahyawijaya, Ziwei Ji, and Pascale Fung. 2023. Negative object presence evaluation (nope) to measure object hallucination in vision-language models. *arXiv preprint arXiv:2310.05338*.
- Long Ouyang, Jeffrey Wu, Xu Jiang, Diogo Almeida, Carroll Wainwright, Pamela Mishkin, Chong Zhang, Sandhini Agarwal, Katarina Slama, Alex Ray, et al. 2022. Training language models to follow instructions with human feedback. *Advances in Neural Information Processing Systems*, 35:27730–27744.
- Fengjun Pan, Xiaobao Wu, Zongrui Li, and Anh Tuan Luu. 2024. [Are LLMs good zero-shot fallacy classifiers?](#) In *Proceedings of the 2024 Conference on Empirical Methods in Natural Language Processing*, pages 14338–14364, Miami, Florida, USA. Association for Computational Linguistics.
- Alec Radford, Jong Wook Kim, Chris Hallacy, Aditya Ramesh, Gabriel Goh, Sandhini Agarwal, Girish Sastry, Amanda Askell, Pamela Mishkin, Jack Clark, Gretchen Krueger, and Ilya Sutskever. 2021. [Learning transferable visual models from natural language supervision](#). *Preprint*, arXiv:2103.00020.
- Hugo Touvron, Thibaut Lavril, Gautier Izacard, Xavier Martinet, Marie-Anne Lachaux, Timothée Lacroix, Baptiste Rozière, Naman Goyal, Eric Hambro, Faisal Azhar, et al. 2023. Llama: Open and efficient foundation language models. *arXiv preprint arXiv:2302.13971*.
- Bin Wang, Fan Wu, Xiao Han, Jiahui Peng, Huaping Zhong, Pan Zhang, Xiaoyi Dong, Weijia Li, Wei Li, Jiaqi Wang, et al. 2023. [Vigc: Visual instruction generation and correction](#). *arXiv*.
- Junfei Wu, Qiang Liu, Ding Wang, Jinghao Zhang, Shu Wu, Liang Wang, and Tieniu Tan. 2024a. [Logical closed loop: Uncovering object hallucinations in large vision-language models](#). In *Findings of the Association for Computational Linguistics: ACL 2024*, pages 6944–6962, Bangkok, Thailand. Association for Computational Linguistics.
- Mingrui Wu, Jiayi Ji, Oucheng Huang, Jiale Li, Yuhang Wu, Xiaoshuai Sun, and Rongrong Ji. 2024b. [Evaluating and analyzing relationship hallucinations in large vision-language models](#). In *Proceedings of the 41st International Conference on Machine Learning*, volume 235 of *Proceedings of Machine Learning Research*, pages 53553–53570. PMLR.
- Xiaobao Wu, Thong Nguyen, and Anh Tuan Luu. 2024c. [A survey on neural topic models: Methods, applications, and challenges](#). *Artificial Intelligence Review*.
- Xiaobao Wu, Thong Thanh Nguyen, Delvin Ce Zhang, William Yang Wang, and Anh Tuan Luu. 2024d. [FASTopic: Pretrained transformer is a fast, adaptive, stable, and transferable topic model](#). In *The Thirty-eighth Annual Conference on Neural Information Processing Systems*.
- Xiaobao Wu, Liangming Pan, William Yang Wang, and Anh Tuan Luu. 2024e. [AKEW: Assessing knowledge editing in the wild](#). In *Proceedings of the 2024 Conference on Empirical Methods in Natural Language Processing*, pages 15118–15133, Miami, Florida, USA. Association for Computational Linguistics.
- Xiaobao Wu, Liangming Pan, Yuxi Xie, Ruiwen Zhou, Shuai Zhao, Yubo Ma, Mingzhe Du, Rui Mao, Anh Tuan Luu, and William Yang Wang. 2024f. [Antileak-bench: Preventing data contamination by automatically constructing benchmarks with updated real-world knowledge](#). *arXiv preprint arXiv:2412.13670*.
- Peng Xu, Wenqi Shao, Kaipeng Zhang, Peng Gao, Shuo Liu, Meng Lei, Fanqing Meng, Siyuan Huang, Yu Qiao, and Ping Luo. 2023. [Lvlm-ehub: A comprehensive evaluation benchmark for large vision-language models](#). *arXiv preprint arXiv:2306.09265*.
- Qinghao Ye, Haiyang Xu, Guohai Xu, Jiabo Ye, Ming Yan, Yiyang Zhou, Junyang Wang, Anwen Hu, Pengcheng Shi, Yaya Shi, et al. 2023. [mplug-owl: Modularization empowers large language models with multimodality](#). *arXiv*.
- Li Yifan, Yifan Du, Kun Zhou, Jinpeng Wang, Wayne Xin Zhao, and Ji-Rong Wen. 2023. [Evaluating object hallucination in large vision-language models](#). In *The 2023 Conference on Empirical Methods in Natural Language Processing*.
- Shukang Yin, Chaoyou Fu, Sirui Zhao, Ke Li, Xing Sun, Tong Xu, and Enhong Chen. 2024. [A survey on multimodal large language models](#). *National Science Review*, 11(12).

Shukang Yin, Chaoyou Fu, Sirui Zhao, Tong Xu, Hao Wang, Dianbo Sui, Yunhang Shen, Ke Li, Xing Sun, and Enhong Chen. 2023. Woodpecker: Hallucination correction for multimodal large language models. *arXiv preprint arXiv:2310.16045*.

Wayne Xin Zhao, Kun Zhou, Junyi Li, Tianyi Tang, Xiaolei Wang, Yupeng Hou, Yingqian Min, Beichen Zhang, Junjie Zhang, Zican Dong, et al. 2023. A survey of large language models. *arXiv preprint arXiv:2303.18223*.

Yiyang Zhou, Chenhang Cui, Jaehong Yoon, Linjun Zhang, Zhun Deng, Chelsea Finn, Mohit Bansal, and Huaxiu Yao. 2024. Analyzing and mitigating object hallucination in large vision-language models. *ICLR*.

Deyao Zhu, Jun Chen, Xiaoqian Shen, Xiang Li, and Mohamed Elhoseiny. 2023. Minigt-4: Enhancing vision-language understanding with advanced large language models. *arXiv*.

Question	Model	Output
	Woodkeeper	There is no sports ball in the image.
Is there a sports ball in the image?	Our	entities: <ul style="list-style-type: none"> • sports ball <ul style="list-style-type: none"> ◦ existing score: 1.0 ◦ attribute score: None ◦ attribute: None relations: None
	Woodkeeper	Yes, there is a table([0.356, 0.532, 0.998, 0.996]) in the image, which can be considered a dining table.
Is there a dining table in the image?	Our	entities: <ul style="list-style-type: none"> • dining table <ul style="list-style-type: none"> ◦ existing score: 0.0 ◦ attribute score: None ◦ attribute: None relations: None
	Woodkeeper	The woman([0.289, 0.066, 0.755, 0.972]) is in the image sitting on a couch([0.154, 0.307, 0.991, 0.908]). However, the specific information does not confirm that the couch is a black leather one.
Is the woman in the image sitting on a black leather couch?	Our	entities: <ul style="list-style-type: none"> • couch <ul style="list-style-type: none"> ◦ existing score: 1.0 ◦ attribute score: 0.9228 ◦ attribute: leather • woman <ul style="list-style-type: none"> ◦ existing score: 1.0 ◦ attribute score: None ◦ attribute: None relations: <ul style="list-style-type: none"> • woman, sit on, couch: 0.9431
	Woodkeeper	Yes, the baby([0.33, 0.366, 0.625, 0.55]) in the image is smiling.
Is the baby in the image smiling?	Our	entities: <ul style="list-style-type: none"> • baby <ul style="list-style-type: none"> ◦ existing score: 1.0 ◦ attribute score: 0.3378 ◦ attribute: smiling relations: None

Figure 3: Examples of inference between Woodpecker and our CutPaste&Find.

Image & Question	Output
 <p data-bbox="328 1043 775 1122">Are there any trees in the image that are not decorated with lights and are located outside of a strip mall?</p>	<p data-bbox="815 707 903 730">entities:</p> <ul data-bbox="847 741 1158 999" style="list-style-type: none"> <li data-bbox="847 741 927 763">• trees <ul data-bbox="895 775 1158 864" style="list-style-type: none"> <li data-bbox="895 775 1126 797">◦ existing score: 1.0 <li data-bbox="895 808 1158 831">◦ attribute score: None <li data-bbox="895 842 1086 864">◦ attribute: None <li data-bbox="847 875 967 898">• strip mall <ul data-bbox="895 909 1158 999" style="list-style-type: none"> <li data-bbox="895 909 1126 931">◦ existing score: 1.0 <li data-bbox="895 943 1158 965">◦ attribute score: None <li data-bbox="895 976 1086 999">◦ attribute: None <p data-bbox="815 1010 919 1032">relations:</p> <ul data-bbox="847 1043 1222 1066" style="list-style-type: none"> <li data-bbox="847 1043 1222 1066">• trees, outside, strip mall: 0.8866
 <p data-bbox="336 1480 775 1536">Are the two women in the image playing table tennis against each other?</p>	<p data-bbox="815 1155 903 1178">entities:</p> <ul data-bbox="847 1189 1158 1447" style="list-style-type: none"> <li data-bbox="847 1189 951 1211">• women <ul data-bbox="895 1223 1158 1312" style="list-style-type: none"> <li data-bbox="895 1223 1126 1245">◦ existing score: 1.0 <li data-bbox="895 1256 1158 1279">◦ attribute score: None <li data-bbox="895 1290 1086 1312">◦ attribute: None <li data-bbox="847 1323 999 1346">• table tennis <ul data-bbox="895 1357 1158 1447" style="list-style-type: none"> <li data-bbox="895 1357 1126 1379">◦ existing score: 1.0 <li data-bbox="895 1391 1158 1413">◦ attribute score: None <li data-bbox="895 1424 1086 1447">◦ attribute: None <p data-bbox="815 1458 919 1480">relations:</p> <ul data-bbox="847 1491 1238 1514" style="list-style-type: none"> <li data-bbox="847 1491 1238 1514">• women, play, table tennis: 0.6176

Figure 4: Failed examples of our CutPaste&Find.

Object	Validation image	Visual-aid images			
wooden medicine cabinet					
VQA score	0.558	0.805	0.383	0.420	
white fridge					
VQA score	0.922	0.737	0.823	0.4973	
train on track					
VQA score	0.655	0.589	0.762	0.845	

Figure 5: Visualization of VQA module on Knowledge base images and test images.